Strength, durability, and microstructure of self-compacting geopolymer concrete produced with copper slag aggregates

Saloni Arora
Southern Cross University Lismore Campus: Southern Cross University
Parveen Jangra (separveenjangra@dcrustm.org)
Deenbandhu Chhotu Ram University of Science and Technology Department of Civil Engineering
https://orcid.org/0000-0002-9896-0274
Yee Lim
Southern Cross University Lismore Campus: Southern Cross University
Thong Pham
Curtin University Bentley Campus: Curtin University

Research Article

Keywords: Self-compacting geopolymer concrete, Compressive strength, Fly ash, Ultrafine slag, Copper slag aggregates

Posted Date: March 16th, 2022

DOI: https://doi.org/10.21203/rs.3.rs-1323386/v1

Abstract

Lack of vibrations on fresh concrete negatively influences the compaction and thus the quality of concrete. This is particularly concerning with geopolymer concrete (GPC) containing sodium silicate (Na 2 SiO 3), which is viscous in nature. In this study, self-compacting geopolymer concrete (SCGC) containing fly ash (FA) and ultrafine slag (UFS) with copper slag aggregates (CSA) was proposed and investigated. CSA were used as a substitute to sand (by weight) in SCGC at different percentages up to 60%. In the fresh state, slump, T500 slump flow, V-funnel, L-box, U-box, and sieve aggregation ratio tests were performed to investigate flowability, passing ability, and viscosity. At the hardened state, the compressive strength, water absorption, chloride ion resistance and sorptivity tests were examined. The flowability of SCGC improved when CSA were added, and the highest slump of 735 mm was achieved for the mix with 60% CSA. Substitution of up to 20% of CSA enhanced the properties of SCGC at all ages. Mix having 20% CSA (20CSA-SCGC) was superior to other mixes, exhibiting the highest compressive strength (47 MPa) at 365 days while possessing the lowest water absorption, sorptivity, and the highest chloride ion resistance. Scanning electron microscopy (SEM) and energy dispersive spectroscopy (EDS) analyses also confirmed the improved microstructure of Mix 20CSA-SCGC. Meanwhile, X-ray diffraction (XRD) analysis confirmed the presence of quartz and calcium silicate hydrate (CSH) products, which were the main contributors to properties enhancement.

Highlights

- Utilization of copper slag aggregates as partial substitution to sand.
- SCGC with improved mechanical and durability properties.
- Microstructure of SCGC studied using SEM, XRD and EDS analyses.
- Correlations between different properties were established.

1. Introduction

Concrete is the second most commonly used material in this modern era, only next to water (Gagg 2014). As per the previous report (Meyer 2004), approximately 10 billion tonnes of concrete is globally produced every year. The production of cement, which is the main binder of concrete, is not only energy-intensive but also environmentally hostile since it is responsible for 5 - 7% of global carbon dioxide (CO_2) emissions (Andrew 2017). Geopolymer concrete (GPC) has been recently suggested (Parveen et al., 2018; Saloni et al., 2021) as a sustainable alternative to conventional concrete, minimizing environmental pollution. GPC utilizes alumina-silicate materials such as fly ash (FA), slag, or rice husk ash (RHA) as binders in place of cement. The utilization of these byproducts, which otherwise would be landfilled, not only resolves the environmental issues related to waste disposal and management but also alleviate the ever-increasing demand for cement production and exploitation of natural aggregates (NA).

Previous studies have shown that GPC exhibits upgraded properties compared to conventional concrete (Dhirendra Singhal and Garg 2017; Jindal et al. 2017). Mechanical performance of GPC produced by other byproducts, such as RHA-based GPC incorporating ultrafine slag (UFS) and corn cob ash, was also studied (Saloni et al. 2021). It was discovered that GPC with improved qualities can be manufactured from waste materials. One of the main shortcomings of GPC is the need for alkaline solutions and elevated temperatures to activate the waste materials. This restricts the application of GPC to the precast industry. To counteract this limitation, the use of slag or UFS, which helps in the setting and hardening process of GPC, has been proposed as a potential solution. The use of slag relaxes the elevated temperature curing requirement of GPC, thus extending its application to cast-in-situ construction. Previous studies have proven that the incorporation of UFS in GPC improved its mechanical and durability characteristics (Parveen et al., 2018; Saloni et al., 2020) due to its excellent binder properties. Some studies reported that the utilization of slag in GPC significantly improved its properties, and GPC is superior to conventional concrete (Dhirendra Singhal and Garg 2017; Jindal et al. 2020; Parveen et al. 2017). Ariffin et al. (Ariffin et al. 2013) studied the effect of sulphuric acid exposure on GPC and conventional concrete and concluded that the GPC outperformed the conventional concrete. In general, previous studies in the literature showed that GPC produced using UFS exhibits improved properties and can be used as sustainable construction materials.

On the other hand, researchers have also suggested the use of copper slag (CS), another type of waste material, to enhance the performance of GPC. CS is the major wastes produced from the copper manufacturing industry. Approximately 2.2 tons of slag is produced for one ton of copper production (Gorai et al. 2003). CS disposal requires a large area of land as dumping ground. On the other hand, the scarcity of natural resources such as sand motivates the use of fine copper slag aggregates (CSA) as a substitute for NA. Previous studies revealed that the properties of GPC improved remarkably with the inclusion of CSA (Singh and Mehta 2020; Yakshareddy et al. 2018). The properties of FA-based GPC produced using CSA were also compared with the properties of conventional concrete, in which GPC showed better performance (Hanio Merinkline et al., 2013). Khan et al. (Khan et al. 2021) studied the characteristics of FA and CS-based geopolymer and the outcomes revealed that CS incorporation improved the performance of geopolymer. FA and CSA were used as substitutes in concrete production, and the findings suggest that using 30% CS instead of fine aggregates improved the mechanical properties (Kumar Tiwary and Bhatia 2021). Prem et al. (Prem et al. 2018) investigated the properties of concrete mixes containing 100% CSA as a substitution for sand. The study concluded that the use of CSA in concrete not only improved mechanical performance but also led to the production of cost-effective, eco-friendly, and sustainable concrete. Sreenivasulu et al. (Sreenivasulu et al. 2020) studied the flexural properties of GPC with CSA. Fine aggregates were substituted with CSA at weight levels of 0, 20, 40, and 60%, and better performance was reported for all substitution levels. Mahendram and Arunachalam (Mahendran and Arunachelam 2016) investigated the characteristics of FA based GPC. Fine aggregates were substituted by CSA up to 100%, with a 10% increase for each mix. The mixtures were cured at 60°C and room temperature using a 14 M NaOH solution. The results revealed that when CSA were introduced into GPC, the compressive strength increased because CSA contributed to enhanced

bonding among various constituents. Several researchers (Al-Jabri et al., 2009, Al-Jabri et al., 2011) demonstrated that CSA incorporation is a viable source for geopolymer synthesis because of its chemical composition, and it can be adopted as a potential replacement of fine aggregates. It is a waste product which is rich in silica and alumina, and have suitable amount of calcium (Ca) that combines with portlandite to produce secondary calcium silicate hydrate (CSH), which helps to the overall strength of materials such as mortar and concrete.

Another typical challenge in field applications of GPC, or concrete in general, is the difficulty associated with proper compaction due to congested reinforcements. The flowability is worsened by the fact that GPC often utilizes sodium silicate (Na_2SiO_3), which is viscous in nature. Self-compacting geopolymer concrete (SCGC) emerges as an excellent solution for achieving the desired compaction, and therefore, sufficient durability for concrete structures. A thorough literature review of the revealed that studies on SCGC produced using UFS with CSA as a replacement for NA are relatively scarce, particularly on the strength and microstructure of SCGC. Because CSA has alumina-silicate properties that make it suitable for use in concrete, including it in SCGC production with UFS and FA as binders could be beneficial for producing sustainable construction materials. There have been no studies that have conducted an in-depth analysis of SCGC characteristics in both fresh and hardened states, as well as its durability performance, which was covered in this investigation. Major factors which affect the properties of self-compacting concrete are passing ability, viscosity, flowability, and segregation resistance. To achieve satisfactory performance based on these factors, the use of alumina-silicate materials, including FA, slag, along with superplasticizer has been proposed. The use of superplasticizer imparts flowability and reduces the viscosity of concrete.

Furthermore, adequate mechanical and durability performance is critical for concrete structures to perform well throughout their service life. This current study utilized both UFS and CSA to develop SCGC. Its strength, durability and microstructural properties were investigated. SCGC mixes were first tested in the fresh state to determine their fresh state characteristics. In the hardened state, the compression test was the main tool used to determine the mechanical performance of the proposed SCGC. Various durability-related tests were also performed, including water absorption, chloride ion resistance and sorptivity tests. The relationship between different parameters was examined using linear regression analysis. Microstructural examinations, including scanning electron microscopy (SEM), energy dispersive spectroscopy (EDS) and X-ray diffraction (XRD) analyses, were also performed to investigate the microstructure of the developed SCGC. Finally, the statistical significance of the experimental research was determined by conducting statistical analysis.

2. Testing Program

2.1. Materials and preparation of specimens

Low Ca FA conforming to Indian standard (IS) 3813 (IS:3812 and BIS 3812 2013) was procured from a coal power plant in New Delhi, India. UFS obtained from the Ambuja cement industry, India was used as

an additive to FA, and as a binder to produce SCGC. CSA were obtained from a copper manufacturing factory in New Delhi, India. The alkaline solution was prepared using Na_2SiO_3 and sodium hydroxide (NaOH) pellets of 98% purity. The chemical compositions of FA, CSA and UFS are summarised in Table 1. Crushed granite and river sand obtained from the Yamuna river, India, were used as NA. The physical properties of various GPC constituents are tabulated in Table 2. The specific gravities for FA, UFS and CSA were 1.90, 2.72, and 3.53, respectively. To determine the grading of sand and CSA, sieve analysis was performed in accordance with American society for testing and materials (ASTM) C136 (American Society of Testing and Materials. 2014) and the particle size distribution curve obtained is shown in Fig. 1. The aggregates were used in saturated surface dry conditions. In this state, the water content of the produced composite is not impacted by the aggregates since the aggregates pore space is completely saturated with water (Gardiner and MacDonald 2013; “Saturated-surface-dry - Wikipedia” 2018), and this state was also most suitable for attaining higher strengths (Teo et al. 2016). The curves obtained were within the specified limits for zone II for aggregates, as mentioned in IS 383: 2016 (Table 9) (IS 383 2016). The XRD study of FA has shown large quartz peaks, mullite, calcite, while the UFS, along with calcite compounds, was found to be an amorphous structure (Saloni et al. 2021).

8M NaOH solution was prepared and cooled for 2 to 3 hours. The literature suggests that optimum GPC properties have been achieved with NaOH solution of 8M (Ng et al. 2018). To prepare the activator solution, NaOH and Na_2SiO_3 were mixed for 5 - 7 minutes, and the mixture was kept at room temperature for 24 hours. The specifications of Na_2SiO_3 are summarised in Table 3. Sand was replaced by CSA (by weight) at different levels of 0, 20, 40, and 60%, and the SCGC mixes were designated as 0CSA-SCGC, 20CSA-SCGC, 40CSA-SCGC, and 60CSA-SCGC, as per the percentage of CSA substitution. Sreenivasulu et al. (Sreenivasulu et al. 2020) and Singh and Mehta (Singh and Mehta 2020) suggested that CSA inclusion in GPC beyond 60% resulted in degradation of properties; therefore, the replacement was limited to 60%. Alkaline activator liquid (AAL) to binder ratio was kept as 0.45, while Na_2SiO_3 to NaOH ratio was fixed at 2.5 as optimum properties were observed with this value in the past study (Khan et al. 2021). The above-mentioned parameters have been decided based on the testing on the trial mixes as these values produced a satisfactory mix with good consistency and also beyond 60% CSA replacement a drastic change in properties was noticed. As for other ingredients (apart from NaOH and Na_2SiO_3), they were initially dry mixed. After the activator solution was added, mixing continued for another four minutes. All specimens were cast and then cured at ambient temperature. Polycarboxylate ether (2.5% of fly ash by weight) was used as the admixture in SCGC to enhance its flowability (Xie and Kayali 2016). Table 4 summarises the detailed compositions of different mixes. The mix design approach was considered following the previous studies (Gupta and Siddique 2020a)(Parveen and Singhal 2017). Admixture was added as 2.5% of binder weight to maintain the flowability of SCGC.s

Table 1: Chemical composition of FA, UFS and CSA (%).

Content (%)	CaO	SiO_2	Al_2O_3	FeO	SO_3	MgO	K_2O	Na_2O
FA	6.57	62.69	26.59	2.56	1.29	1.16	0.18	0.12
UFS	34.94	36.64	19.38	1.71	0.14	5.87	0.92	0.40
CSA	3.44	32.55	4.13	54.73	1.44	1.62	1.27	0.82

Table 2: Physical properties of SCGC constituents.

Materials	Appearance	Specific gravity	Fineness modulus	Water absorption (%)	Unit weight (kg/m^3)
River sand	Grey	2.61	2.25	3.15	1245
Coarse aggregates	–	2.67	6.21	1.28	1685
FA	Light greyish	1.9	-	-	1170
UFS	Blackish	2.72	-	-	1020
CSA	Black, Glassy texture	3.53	3.15	0.42	2000

Table 3: Sodium silicate specifications.

Property/Constituent	Appearance
Colour	Colourless
Sodium oxide (Na_2O)	16.30 (%)
Silica (SiO_2)	33.95 (%)
Modulus (SiO_2: Na_2O)	2.08
Total solids	50.25 (%)
Water	49.75 (%)

Table 4: Mix design of SCGC.

Mix	0CSA-SCGC	20CSA-SCGC	40CSA-SCGC	60CSA-SCGC
FA (kg/m^3)	375	375	375	375
UFS (kg/m^3)	125	125	125	125
Sand (kg/m^3)	970	776	582	388
CSA (kg/m^3)	0	194	388	582
Coarse aggregates (kg/m^3)	780	780	780	780
AAL (kg/m^3)	225	225	225	225
NaOH (kg/m^3)	64.29	64.29	64.29	64.29
Na_2SiO_3 (kg/m^3)	160.71	160.71	160.71	160.71
Admixture (%)	2.5	2.5	2.5	2.5

2.2. Testing of specimens

The slump of various mixes was determined according to ASTM C143 (ASTM C143/C143M 2015). The slump cone tests are commonly used to examine the workability, a property that describes the efforts required to manipulate a specific amount of freshly mixed concrete with minimal homogeneity loss. V-funnel, L-box, U-box, and sieve aggregation tests were performed following the European standards "*The European Guidelines for Self-Compacting Concrete Specification, Production and Use "The European Guidelines for Self Compacting Concrete,"* (2005) and *Specification and Guidelines for Self-Compacting Concrete* (2002) to determine the fresh properties of SCGC, such as flowability, passing ability, viscosity, and segregation resistance. For slump cone and T500 slump flow testing, a cone dimensioned 100 × 200 × 300 mm was adopted, and concrete was poured in three layers, followed by lifting the cone vertically and allowing concrete to flow. The height difference (difference between the top of the slump cone and concrete surface) was concluded as slump. The time taken by concrete to reach a 500 mm mark was reported as T500 slump flow. In the V-funnel test, a V-shaped funnel is filled with concrete, and the time taken for emptying was noted. Ideally, the flow time should be between 8 and 12 seconds (*Specification and Guidelines for Self-Compacting Concrete* 2002). A L-box with a horizontal flow tank and a vertical hopper with a gate at its bottom was used for L-box testing. Concrete was initially filled in the vertical hopper, and then the bottom gate was opened after a min. The difference in heights of the horizontal concrete surfaces was measured, and the ratio of these heights was referred to as passing ratio. A U-shaped apparatus was used for the test, and concrete was filled in the left apartment, and the apparatus was left to stand for 1 min. The gate was then left, and concrete flowed to the other side. The filling height was noted as the difference between the heights of the concrete surface in the two compartments.

In the hardened state, compression tests on cylinders (150 × 300 mm) were performed using a compression testing machine according to ASTM C39 (ASTM International 2020) requirements at 7, 28,

90, and 365 days of age. Water absorption and volume of permeable voids tests were performed using standard ASTM C642-13 (ASTM C642-13 2013) to assess the permeability of SCGC specimens. The resistance against chloride attack was investigated using the rapid chloride permeability test (RCPT) according to guidelines of ASTM C1202 (ASTM C1202 2012). Before being placed in the RCPT migration cells, the specimens were vacuum-saturated in the RCPT. The resistance of the concrete specimen to chloride ions is related to the total charge transmitted. Sorptivity tests were conducted in accordance with the guidelines of ASTM1585 (ASTM C1585-13 2013). These tests were conducted at the ages of 28, 90 and 365 days, and the average value of the results of three specimens was reported as the final value. The specimens were demolded after 36 hours of casting followed by curing at room conditions with relative humidity of 60% and temperature of (25±2)°C. At the desired testing age, the tests were performed.

After performing the compression tests on the fractured specimens from the inner core of SCGC, SEM and EDS analysis were conducted to investigate the microstructure of SCGC. A scanning electron microscope was used, and the sample was placed inside the chamber. After that, a focused beam of electrons was generated to strike the sample, and the SEM images were displayed on a computer screen. The powder collected from the damaged specimens was also subjected to XRD analysis. For XRD testing, the sample was irradiated with X-rays, and a graph between scattering angles and the intensities of X-rays emitted was obtained. Statistical package for the social sciences (SPSS) version 20 was used to conduct statistical analysis on the results obtained.

3. Results And Discussion

3.1. Fresh stage properties

The results of fresh stage properties of SCGC mixes are summarised in Table 5. An enhancement in flowability, passing ability and viscosity was noticed when CSA were used in SCGC. The range of slump was observed as 675 - 735 mm for SCGC mixes. As mentioned above, CSA have a glassy nature (Mavroulidou 2017a), which enhanced the flowability and increased the workability of SCGC mixes. The highest slump was identified for Mix 60CSA-SCGC (735 mm), while the lowest slump was for Mix 0CSA-SCGC (675 mm). Meanwhile, T_{500} slump flow and V-funnel time reduced with the increment of CSA in SCGC. CSA have low water absorption (0.42%), which led to a reduced T_{500} slump because of the release of excess water, which formed a non-homogeneous mix with a higher probability for bleeding and segregation.

For the control mix (0CSA-SCGC), V-funnel time was 7.48 s, and it decreased when the CSA content increased. A reduction of 34.2% was observed for Mix 60CSA-SCGC compared to the control mix. The cause for this phenomenon was the lower viscosity of SCGC mixes when CSA were added. Viscosity influences the consistency and causes variation in the flowing time, a mix with low viscosity can flow easily. Based on the slump flow, the mixes were classified under category SF2 (slump flow class); while they were in category VF1 (viscosity class) on the basis of V-funnel time (*The European Guidelines for*

Self-Compacting Concrete Specification, Production and Use "The European Guidelines for Self Compacting Concrete" 2005). The range of passing ratios for SCGC mixes was 0.78 - 0.98, indicating that the CSA substitution enhanced the passing ability of SCGC mixes.

The U-box values varied between 15 - 20 mm, which further confirmed the increase in the passing ability of SCGC mixes, as also reported in the previous study (Gupta and Siddique 2020b). For Mix 0CSA-SCGC, the difference in filling height was 20 mm; it decreased to 15 mm for Mixes 20CSA-SCGC and 40CSA-SCGC. For Mix 60CSA-SCGC, an increase in filling height difference was noticed (18 mm). As CSA particles were heavy, they settled easily at the bottom of the U-box and increased the filling height. Also, for mixes with more than 40% CSA, chances of segregation and bleeding were higher due to the glassy nature and low water absorption of CSA particles.

The sieve aggregation ratio fluctuated from 3.65 - 11.75 when the CSA content increased from 0 to 60%. All values recorded were lower than 15%, which lies within the acceptable range according to (*The European Guidelines for Self-Compacting Concrete Specification, Production and Use "The European Guidelines for Self Compacting Concrete"* 2005). The combined action of FA, UFS, and the filler action of CSA were responsible for the enhancement in properties in the fresh stage since they provided a binder effect, thus forming a more homogeneous mix, as also evident from Fig. 7. FA and UFS as binders significantly support the matrix development by filling up the matrix pores and creating a compact matrix. Therefore, it can be concluded that the CSA substitution up to 60% has no adverse effect on the fresh properties of SCGC, and satisfactory properties can be attained.

Table 5: Properties of fresh SCGC.

Mixes	0CSA-SCGC	20CSA-SCGC	40CSA-SCGC	60CSA-SCGC
Slump (mm)	675	710	720	735
T_{500} slump flow (s)	3.05	2.28	1.65	1.20
V-funnel (s)	7.48	6.65	5.68	4.92
Passing ratio	0.78	0.83	0.92	0.98
U-box (mm)	20	15	15	18
Sieve segregation ratio (%)	3.65	5.45	9.70	11.75

3.2. Hardened stage properties

3.2.1. Compressive strength

The compression tests were performed at the age of 7, 28, 90 and 365 days, and the results are shown in Fig. 2. An increase in the compressive strength was observed with 20% CSA substitution. The 28-days compressive strength of the control mix was 34.38 MPa, and it increased to 37.42 MPa for Mix 20CSA-

SCGC. However, when the CSA content increased beyond 20%, the trend reversed, and the compressive strength decreased. The lowest value was recorded for Mix 60CSA-SCGC (33.10 MPa).

Similar to conventional concrete, the compressive strength increased with age. Yet, the extent was insignificant beyond 90 days (only 2 - 7% increment was identified at 365 days with respect to 90 days). The 90-day compressive strength was in the range of 41 - 46 MPa, while the 365-day compressive strength varied between 44 - 48 MPa. The largest increase was recorded between the age of 7 to 28 days (58 - 86%). At all curing ages, the lowest compressive strength was observed for Mix 60CSA-SCGC, while the highest compressive strength was achieved by Mix 20CSA-SCGC. It is interesting to note that, even at 60% CSA substitution, the compressive strength remained marginally higher than the control mix. This implies that up to 60% CSA substitution, there is no detrimental effect on the compressive strength of concrete.

The increase in compressive strength can be explained by the binder action of UFS and interlocking effect of CSA (Al-Jabri et al. 2011), which resulted in the formation of additional Ca products, acting as fillers to create a denser microstructure and thus increased the compressive strength of SCGC mixes. Furthermore, the ultrafine size of the UFS particles, again acting as a filler and leading to the generation of Ca -based products, reduced the chances of air penetration into SCGC, which could decrease the mix density and weaken the matrix structure.

The decrease in the compressive strength beyond 20% CSA substitution, on the other hand, can be attributed to inadvertent excess water in SCGC due to the presence of CSA, which has very poor water absorption (0.48%). The excess water increased the water to cement ratio of the mix and decreased the stability of the SCGC matrix due to a higher risk of bleeding and segregation, which eventually led to the strength decrease. One possible solution is to reduce the water-cement ratio for mix with higher CSA content, as CSA absorbs less free water in the mix. This could potentially create a mix with a similar slump yet possessing compressive strength similar to or higher than the reference mix.

The above observations generally agreed with previous studies. An enhancement in the compressive strength was noticed for FA-based GPC produced using CSA by Mahendran and Arunachelam (Mahendran and Arunachelam 2016). With 100% CSA substitution, the compressive strength of 40.7 MPa was obtained under ambient curing. However, the highest compressive strength was obtained at 60% substitution. Also, higher strength was obtained, when CSA content was increased in GPC, and the lowest strength was noticed for the control mix (30.08 MPa). The variation in the results, when compared to the current study, can be attributed to the difference in the interaction between different GPC ingredients. The testing conditions also varied and thus resulted in different interactions based on the ingredients, proportions, temperature and humidity conditions due to the lack of standard provisions for GPC (Imtiaz et al., 2020).

On the other hand, the effects of NaOH concentration and CSA substitution on the properties of GPC were studied by Rathanasalam et al. (Rathanasalam et al. 2020). CSA were used as a complete substitution of sand with NaOH solution of 10, 12 and 14M. Higher compressive strength was obtained when CSA were

used in place of sand. An increase of 12.35% in 3-day compressive strength by GPC mix produced using 12M NaOH solution and 15% slag was achieved, in comparison with compressive strength of the reference mix. Merinkline et al. (Hanio Merinkline et al., 2013) also noticed an overall improvement in the compressive strength of concrete (6.36% increase in 28-day strength) when sand was replaced with CSA. The findings of the previous studies generally aligned well with the results of the current study, with only minor variation due to different interactions between different constituents.

3.2.2. Water absorption

The water absorption test measures the amount of water absorbed by SCGC mixes as well as the volume of permeable voids in SCGC, which is a crucial durability parameter. Fig. 3 depicts the experimental results of the water absorption experiments. In general, the water absorption of concrete decreased with age as the microstructure and properties of the SCGC matrix improved.

At 28^{th} day, the water absorption was in the range of 6 - 8%. The lowest water absorption was noticed for Mix 20CSA-SCGC, while the highest water absorption was observed for the control mix. This trend was observed at all ages. At 365^{th} day, the lowest water absorption was 5.08%, while the highest water absorption was 5.83%, indicating a reduction of the water absorption. When the CSA content increased from 0 to 20%, the water absorption decreased (11 - 13% for various ages), while with further substitution, a reverse trend was observed. The highest decrease in water absorption was 12.58%, occurring at the age of 28 days with respect to water absorption at 7 days. The decrease can be related to pore reduction due to enhancement in the microstructure because of binding properties imparted by FA, UFS and CSA (provided interlocking effect as can be seen from Fig. 7). However, the free water content in SCGC increased with further substitution of CSA due to its low water absorption and glassy surface, which increased the number of voids in the SCGC matrix (refer to Fig. 7 (c)) and thus increased the water absorption. At 60% CSA substitution, the values were similar to the control mix. This trend of the water absorption was similar to that of the compressive strength, and the change of the microstructure was responsible for these two properties.

In addition to water absorption, volume of permeable voids was also obtained, as presented in Fig. 4. The highest permeable voids volume (13.11%) was observed for the control Mix (0CSA-SCGC) at 28 days; it reduced to 11.46% for Mix 20CSA-SCGC. At 90^{th} and 365^{th} days, the lowest values achieved were 10.37 and 8.64% (for Mix 20CSA-SCGC), respectively. These results can also be also related to the compressive strength of SCGC mixes. The denser and compact microstructure for mix with 20% CSA (refer to Fig. 7 (b)) had fewer voids compared to other mixes and, therefore, lower water absorption and volume of permeable voids.

Previous studies also reported similar observations. A reduction in water absorption was observed due to CSA substitution up to 20% was reported by Gupta and Siddique (Gupta and Siddique 2020b). CSA were used at substitution levels of 0 - 40% for sand, and after 20% substitution, an increment of 10% in water absorption was noticed for each consecutive mix. In another study by Al-Jabri et al. (Al-Jabri et al. 2011),

the water absorption was found to reduce with the inclusion of CSA in concrete (up to 50% of CSA content); but with further CSA substitution, the value increased. These findings supported the results of the current investigation. However, due to the different interaction mechanisms of various concrete ingredients and mix designs, some variations are expected. Previous studies (Sivaranjani S and Sridhar M, 2019; Un, 2017) have shown that GPC and traditional concrete behaved similarly, it is thus reasonable to compare such concrete based results with the GPC based findings in this study.

3.2.3. Chloride ion resistance

The RCPT values were obtained at the age of 28, 90, and 365 days, and the results are shown in Fig. 5. The range of RCPT values at 28 days was 963 - 1293 Coulombs, with Mix 20CSA-SCGC and Mix 0CSA-SCGC recorded the highest and lowest values, respectively. At 90 days, the values decreased to 590 - 955 Coulombs, which further reduced at 365 days to 394 - 672 Coulombs. At all ages, the lowest RCPT values were observed for Mix 20CSA-SCGC.

When the CSA content increased beyond 20%, the RCPT values started to increase, which indicates a reduction in resistance to chloride ion penetration. The reasons for this decrease are: (1) the combined filling action of UFS and CSA, which reduced the air content in the matrix structure and thus strengthened its microstructure; and (2) the additional binding effect due to UFS and CSA resulted in a denser microstructure. The outcome was a reduction in RCPT values. However, when the CSA content increased beyond 20%, a degradation in the microstructure was expected, leading to an increase in the number of voids. This provided an easy passage for the penetration of chloride ions, which increased the probability of chloride-induced corrosion. Thus, to ensure satisfactory durability performance against chloride attack, the CSA content in SCGC should be limited to 20%. In addition, with an increase in age, chloride ion penetration resistance also increased, as indicated by the decreasing RCPT values. Once again, the improvement in microstructure with age contributed to greater resistance.

Lower RCPT values are critical to ensure durability performance in the longer term, and it also relates to water absorption and compressive strength. A higher RCPT value also indicates a higher water absorption and poor compressive strength. As per ASTM C1202 (ASTM C1202 2012), the RCPT values of Mix 20CSA-SCGC of all ages were classified as ‘very low’, while for mixes with 40% and 60% of CSA, the RCPT values were considered ‘low’ at 28 days and ‘very low’ at 90 and 365 days.

The classification of chloride penetration resistance based on the charge passed was done in accordance with ASTM C1202 (ASTM C1202 2012) guidelines, as shown in Table 6. According to the measured charge passed, the probability of chloride penetration for Mix 20CSA-SCGC fell under the ‘very low’ category (at all ages).

Chloride ion resistance of GPC mixes produced using CSA as a substitution to sand was studied by Sivaranjani and Sridhar (Sivaranjani S and Sridhar M, 2019). The results concluded that CSA substitution reduced the chances of chloride attack and provided satisfactory results from durability’s perspective.

Similar results were also reported by Rohith and Elavenil (Rohith et al. 2018). In short, the outcomes of the present study are validated by similar previous studies as mentioned above.

Table 6: Classification of chloride permeability based on total charge passed (ASTM C1202, 2012).

Charge passed (Coulombs)	>4000	2000 - 4000	1000 - 2000	100 - 1000	<100
Chloride ion permeability range as per ASTM C1202	High	Moderate	Low	Very low	Negligible

3.2.4. Sorptivity

Sorptivity test was conducted to determine the resistance of GPC against water permeation in the unsaturated state. Factors affecting sorptivity are aggregates characteristics, mix proportion, admixture type and placement method. The results of the sorptivity test are displayed in Fig. 6. In comparison with the control mix, the sorptivity coefficient significantly decreased when 20% of CSA were added as a result of filler action and additional reactions of UFS and CSA. With further substitution, the sorptivity coefficient started to increase again. For the control mix (0CSA-SCGC), sorptivity coefficient at 28 days was 0.0061 mm/sec$^{1/2}$, which decreased to 0.0049 mm/sec$^{1/2}$ for Mix 20CSA-SCGC and increased to 0.0059 mm/sec$^{1/2}$ for Mix 60 CSA-SCGC.

Similar to the previous observations, the sorptivity coefficient decreased with an increase in curing ages due to improved matrix structure, which lowered the chances of water permeation. At 90 days, the sorptivity coefficient was in the range of 0.0039 - 0.0052 mm/sec$^{1/2}$, while at 365 days, the range was further reduced to 0.0036 - 0.0043 mm/sec$^{1/2}$. The decrease in the sorptivity coefficient of Mix 20CSA-SCGC at the ages of 28, 90, and 365 days was 19.67, 25, and 16.27% in comparison with the control specimen, respectively. Even at 60% CSA substitution, the sorptivity coefficients remained slightly lower than the control mix.

The reason for the reduction in sorptivity can again be related to the enhancement in the pore structure of SCGC matrix due to the presence of FA, UFS and CSA, which acted as filler materials and additional reaction products (Ca -based). Large and permeable pores were partially filled by additional Ca products produced by UFS and CSA, resulting in smaller and non-permeable pores (Al-Jabri et al. 2011; Jindal et al. 2017). A denser GPC matrix was also formed with increasing age due to further Ca -based products. The results can also be directly related to the results of water absorption.

A reduction in sorptivity was reported by Mathew and Usha (Mathew and Usha 2016) when CSA were incorporated in GPC as a partial substitution to sand. The results of the current study are also consistent with the results of (Gupta and Siddique 2020b). Sand was replaced with CSA at various levels (i.e., 10, 20, 30, 40, 50 and 60%), and the water absorption of specimens was found to decrease up to 20% CSA substitution. Meanwhile, specimens with higher CSA substitution levels (>20%) resulted in higher water absorption with respect to the reference mix. These results are consistent with the present results.

4. Microstructure

4.1. SEM and EDS analysis

SEM analysis was conducted to determine the morphology of SCGC matrix. The SEM images show changes in the microstructure of the SCGC mixes. The compressive strength and other properties of SCGC mixes can be closely related to their microstructure. The microstructure of SCGC mixes at the age of 90 days is presented in Figs. 7 (a - d). Lower strength and weaker SCGC properties were observed for Mix 60CSA-SCGC due to the presence of cracks and voids. As shown in Fig. 7, needle-shaped ettringites were observed in the control Mix (0CSA-SCGC). When the CSA content increased to 20%, the production of CSH and calcium aluminate silicate hydrate (CASH) gels increased significantly, which was primarily responsible for the improved properties of Mix 20CSA-SCGC along with sodium aluminate silicate hydrate (NASH) gel. A compact and refined structure with fewer voids was observed as FA, UFS, and CSA filled the voids. No ettringites were observed, and clear layers of CASH were observed.

When the CSA content increased to 40%, the formation of ettringite needles was again observed. The same was observed for Mix 60CSA-SCGC. The water absorption of CSA were very low (0.48%), resulting in the release of excess water, void formation, and a reduction in strength, especially for Mix 60CSA-SCGC. This is supported by the experimental results presented above, which supported the fact that Mix 60CSA-SCGC was inferior to other SCGC mixes.

To study the composition of various elements in SCGC mixes, EDS analysis was conducted, and the findings are shown in Table 7. The elements observed in major proportions were Oxygen (O), Ca, Si (Silicon), Al (Aluminium), and Mg (Magnesium). Furthermore, other elements including, Potassium (K), Sodium (Na), and Iron (Fe) were found as well but in minor proportions. For all the SCGC mixes, Ca/Si ratio was also evaluated and was correlated to the compressive strength, as recommended by Gupta and Siddique (Gupta and Siddique 2020b). Ca/Si ratios for Mixes 0CSA-SCGC, 20CSA-SCGC, 40 CSA-SCGC, and 60CSA-SCGC were 1.87, 1.40, 1.93, and 1.82, respectively. The lowest Ca/Si ratio was observed for Mix 20CSA-SCGC (1.40), which exhibited the highest strength. A previous study by (Guru Jawahar et al. 2013) has found that the decrease in Ca/Si ratio can be correlated to the reduction of the microcracking width and thus leading to the improved microstructure of the mix. As a result, Mix 20CSA-SCGC with the lowest Ca/Si ratio had the highest compressive strength. As can be seen from Table 7, Mix 20CSA-SCGC had the highest Ca content, which led to the formation of additional Ca products and thus improved the compressive strength and other properties. The microstructure showed a dense matrix because of the dissolution of Al and Si from CSA (angular shape). Due to CSA, a stronger matrix with excellent bonding among various components was identified.

In addition, though the previous studies suggested that Na/Si ratio should vary from 0.80 – 1.20 for geopolymer formation (Khan et al. 2021), different values were noticed in the current study. This disparity could be due to the interaction of various SCGC ingredients; however, acceptable characteristics were achieved. The highest Si/Al ratio was recorded for Mix 20CSA-SCGC (7.48), and the literature indicated that this would produce more compact and homogeneous microstructures (Khan et al. 2021).

Table 7: EDS analysis of SCGC mixes at 90 days.

Chemical elements (Atomic %)	0CSA-SCGC	20CSA-SCGC	40CSA-SCGC	60CSA-SCGC
O	76.24	71.47	75.25	74.02
Ca	12.95	14.86	13.2	14.72
Si	6.91	10.62	6.84	8.11
Al	1.22	1.42	1.71	1.63
Mg	0.89	0.44	0.77	0.75
K	0.52	0.51	0.95	0.24
Na	0.62	0.22	0.72	0.16
Fe	0.65	0.46	0.56	0.37
Ca/Si	1.87	1.4	1.93	1.82
Na/Si	0.09	0.02	0.11	0.02
Si/Al	5.66	7.48	4.00	4.98

4.2. XRD analysis

To investigate the phases formed in the SCGC mixes, XRD analysis was conducted at 90 days, and the results are shown in Fig. 8. It can be observed that crystalline phases existed in the SCGC mixes. Also, there was no major change in phases, with the increase in CSA% from 0 to 60%. A significant peak of quartz was observed in all the SCGC mixes. It has a hexagonal crystalline structure. Quartz facilitated the manufacture of high-strength concrete (as it facilitated a reduction in mix porosity (Mosaberpanah and Eren 2017)) and enhanced performance. In addition, quartz could effectively pack at the surface of the aggregates, resulting in an extremely compact interfacial transition zone (ITZ) with no apparent pores, hence a higher strength (Mayhoub et al. 2021). This also supported the enhancement in strength, when CSA were incorporated into SCGC.

The other phases observed were calcium hydroxide, anorthite, calcite, merwinite, CSH, and nepthaline. For Mix 60CSA-SCGC, phase of aluminium silicate hydrate (ASH) was also observed (it was not seen in other SCGC mixes). It led to the release of heat and the formation of cracks, which caused strength reduction and degradation in properties. The release of excess heat was observed during the mixing process. This phenomenon could be the main cause of crack formation, and it could be related to the microstructure of Mix 60CSA-SCGC, where cracks were observed, as shown in Fig. 7.

5. Establishing Correlation Between Various Parameters

5.1. Relationship between flow properties

Linear regression is a tool used to establish the relationship between different parameters. It can predict the value of one variable based on the value of another variable. To figure out the relationship between flowability, passing ability, viscosity and segregation resistance of SCGC mixes, linear regression was performed. The regression coefficient (R^2) values for the relationships of slump with T_{500} slump flow and slump with V-funnel time were 0.96 and 0.91, respectively, as shown in Fig. 9. The correlations were strong, based on R^2 values. With the increase in slump, a decrease in T_{500} slump flow was noticed, which also validates the relationship of flowability and viscosity of SCGC mixes. The slump and V-funnel time exhibited an inverse relationship.

The relationships between V-funnel time, passing ratio, and slump flow were also plotted, as shown in Fig. 10. The R^2 values for the correlation between (1) V-funnel time with passing ratio and (2) V-funnel time with slump were 0.99 and 0.91, respectively. An inverse relationship was observed between V-funnel time with passing ratio and V-funnel time with slump. Behera et al. (Behera et al. 2019) also observed a similar inverse relationship between slump with T_{500} slump flow and slump with V-funnel time. A strong correlation was observed for V-funnel time with passing ratio (with R^2 of 0.97) by Gupta and Siddique (Gupta and Siddique 2020b). The results of the studies mentioned above align with the outcomes of the current investigation.

Knowing the independent variable, the derived equations can be used to estimate the other variables. However, these were obtained based on the range of values observed in the current study; the possibility of extrapolation into other cases was not investigated in this study.

To determine the accuracy of the predicted equations, a comparison was made between the predicted values, the experimental results, and the previous literature. Fig. 11 shows the relationships between slump, T_{500} slump flow and V-funnel time. Since no literature on SCGC generated using UFS and FA as binders and CSA as fine aggregates substitute is reported, for comparison with past literature, a study conducted on self-compacting concrete by Gupta and Siddique (Gupta and Siddique 2020b) has been used. The experimental and projected findings only exhibited a minor variation, implying that regression equations are accurate. Furthermore, the findings from the prior study agreed well with the present results, which justified the validity of the current study.

5.2. Relationship between properties at hardened state

Linear regression analysis was again performed to examine the relationship between different hardened state properties. Only those relationships with a satisfactory relation (high R^2) were included in this study. The relationships obtained for RCPT values with water absorption and compressive strength of various SCGC mixes are depicted in Fig. 11. The 28-day values of the parameters were used for developing the relationships. An inverse relationship was observed between RCPT values and compressive strength (R^2 = 0.83); however, a direct relationship was identified between RCPT values and water absorption (R^2 = 0.98). With an increase in the charge passed, compressive strength declined, and water absorption increased.

Increment in charge passed implied a matrix with more voids, which would also absorb more water due to its loose and non-compact structure. This was also related to the increased rate of water absorption, i.e., sorptivity. Further, a poor matrix with lower strength would allow a higher proportion of chloride ions to enter it, which raised the charge passed and hence an inverse relationship between compressive strength and charge passed was identified.

6. Statistical Analysis

Statistics are used in research to make more scientific judgments. It is based on gathering, analyzing, and displaying massive volumes of data in order to find underlying patterns and trends. Statistical analysis of various parameters helps in understanding the relativity of various parameters and their distribution in the database. It facilitates determining the level of confidence in the findings (“Benefits of Statistical Modeling – Test Science,” 2015.). For knowing the significance of the experimental tests, Analysis of Variance (ANOVA) method was adopted to process the experimental data. The statistical effect of different percentages of CSA on various SCGC mixes at different curing ages was investigated. The significance level was fixed as 0.05 for the ANOVA test. Dependent variables were percentage levels of CSA, i.e., 0, 20, 40, and 60%, while curing ages were selected as independent variables. If the p-value (significance) was less than or equal to 0.05, the results were considered statistically significant.

The average compressive strength was considered for the statistical analysis. At all curing ages, the compressive strength was statistically significant as expected. In addition, the Post Hoc Turkey test was used to compare different strengths at various curing ages, and the results are summarised in Table 8.

Furthermore, the water absorption, RCPT values and sorptivity were also compared using the ANOVA test. The dependent variables were the durability properties, while the curing ages were considered as independent variables. Significant statistical results were noticed for the durability parameters as p-value was less than 0.05 at all ages. Post Hoc Turkey test was again used to perform multiple comparisons, and the average values of durability parameters were compared. The results of the Post Hoc test for durability properties are tabulated in Table 9. At all curing ages, statistically significant results were observed as indicated from p-values.

The findings of this study were also compared to those of other investigations. Statistical analysis was performed by Mavroudilou (Mavroulidou 2017b) to determine the relevance of compressive strength in relation to crucial elements such as water to cement ratio, cement type, and CSA content in the concrete mix. Apart from the ANOVA test, Kruskal-Wallis analysis was also performed. The water to cement ratio was identified as the most significant factor, as observed from the ANOVA test, and the other important factor affecting compressive strength was the type of cement. The theoretical and experimental findings also confirmed this (“Effect of Water Cement Ratio on Strength of Concrete – we civil engineers,” 2017.; Rahmani et al., 2012). However, CSA were found to have no statistical significance. Similar results were obtained by Kruskal-Wallis analysis. As for conventional concrete, the most significant factor governing its compressive strength is water to cement ratio. In GPC, water to binder ratio is the main parameter

governing the compressive strength (Xu and Shayan 2016). Therefore, it is suggested that less water should be used in the case of a high substitution level of CSA to reduce excessive water in the mix due to low water absorption of CSA.

Table 8: Comparisons of compressive strength by Post Hoc Tukey method.

Dependent variable	(P) mix	(Q) mix	Significance
0	7 days	28 days	0.000*
		90 days	0.000*
		365 days	0.000*
	28 days	7 days	0.000*
		90 days	0.000*
		365 days	0.000*
	90 days	7 days	0.000*
		28 days	0.000*
		365 days	0.389
	365 days	7 days	0.000*
		28 days	0.000*
		90 days	0.389
10	7 days	28 days	0.000*
		90 days	0.000*
		365 days	0.000*
	28 days	7 days	0.000*
		90 days	0.002*
		365 days	0.000*
	90 days	7 days	0.000*
		28 days	0.002*
		365 days	0.134
	365 days	7 days	0.000*
		28 days	0.000*
		90 days	0.134
20	7 days	28 days	0.000*
		90 days	0.000*
		365 days	0.000*
	28 days	7 days	0.000*

		90 days	0.000*
		365 days	0.000*
	90 days	7 days	0.000*
		28 days	0.000*
		365 days	0.570
	365 days	7 days	0.000*
		28 days	0.000*
		90 days	0.570
30	7 days	28 days	0.000*
		90 days	0.000*
		365 days	0.000*
	28 days	7 days	0.000*
		90 days	0.000*
		365 days	0.000*
	90 days	7 days	0.000*
		28 days	0.000*
		365 days	0.584
	365 days	7 days	0.000*
		28 days	0.000*
		90 days	0.584

Table 9: Statistical significance of various durability parameters.

Statistical significance of durability parameters.

Dependent variable	(I) mix	(J) mix	Significance		
			Water absorption	RCPT values	Sorptivity
0	28 days	90 days	0.012*	0.000*	1.000
		365 days	0.000*	0.000*	0.000*
	90 days	28 days	0.012*	0.000*	1.000
		365 days	0.014*	0.000*	0.000*
	365 days	28 days	0.000*	0.000*	0.000*
		90 days	0.014*	0.000*	0.000*
10	28 days	90 days	0.102	0.000*	1.000
		365 days	0.004*	0.000*	0.000*
	90 days	28 days	0.102	0.000*	1.000
		365 days	0.120	0.000*	0.000*
	365 days	28 days	0.004*	0.000*	0.000*
		90 days	0.120	0.000*	0.000*
20	28 days	90 days	0.022*	0.000*	1.000
		365 days	0.008*	0.000*	0.000*
	90 days	28 days	0.004*	0.000*	1.000
		365 days	0.001*	0.000*	0.000*
	365 days	28 days	0.008*	0.000*	0.000*
		90 days	0.070	0.000*	0.000*
30	28 days	90 days	0.033*	0.000*	1.000
		365 days	0.002*	0.000*	0.000*
	90 days	28 days	0.033*	0.000*	1.000
		365 days	0.041*	0.000*	0.000*
	365 days	28 days	0.002*	0.000*	0.000*
		90 days	0.142	0.000*	0.000*

Note: p value < 0.05 (significant).

7. Conclusions

The current study reports the investigation of various SCGC with CSA as a partial substitution to sand. The results showed that the combined binder and interlocking effects of UFS and CSA, respectively, increased the strength and durability of SCGC, with the optimum results obtained when 20% CSA replacement was adopted. Based on the key experimental findings, the following conclusions can be drawn:

1. The flowability properties of SCGC were improved by increasing the CSA content. Mix 60CSA-SCGC showed the highest slump (735 mm). The combined influences of UFS and CSA improved the passing ability of the SCGC mixes, making compaction easier.
2. The experimental outcomes revealed that 20% CSA were the optimal value of CSA substitution since Mix 20CSA-SCGC had the highest compressive strength (47.03 MPa at 365 days), the lowest water absorption, charge passed and sorptivity. This enhancement in performance can be attributed to the denser and more compact microstructure of Mix 20CSA-SCGC. This was achieved through the formation of additional Ca products due to UFS and CSA addition. However, further increase in CSA level led to an excess water release and a weaker matrix microstructure and, therefore, a degradation in properties.
3. It was found in the microstructure study that, up to a CSA substitution of 20%, CSH gel was formed due to the coexistence of UFS and CSA, which led to the filling of voids and the formation of a compact and dense matrix structure. Cracks were noticed when the CSA content was increased beyond 20%, resulting in a matrix structure with a higher void volume and lower strength. Also, Ca/Si ratio was the lowest for Mix 20CSA-SCGC, as obtained from EDS analysis, and it implies higher strength. As expected, Mix 20CSA-SCGC exhibited the highest compressive strength from the compression tests.
4. Statistical relationships between various parameters were determined, and a strong statistical relationship was found between fresh properties, compressive strength, and durability parameters.

In conclusion, the results of this study indicated that sand can be substituted by CSA in order to produce sustainable SCGC with FA and UFS as binders. The SCGC produced possessed satisfactory properties for use in on-site construction purposes.

Declarations

Ethical Approval, Consent to Participate and Consent to Publish: Not applicable.
Authors Contributions:

Saloni Arora: Conceptualization, Software, Data curation, Writing- Original draft preparation.

Parveen Jangra: Data curation, Writing, Methodology, Visualization, Investigation, Supervision, Reviewing and Editing.

Yee Yan Lim: Funding acquisition, Writing, Software, Reviewing and Editing, Supervision.

Thong M. Pham: Funding acquisition, Writing, Reviewing and Editing.

Funding

No funds, grants, or other support were received during the preparation of this manuscript.

Competing Interests

The authors have no relevant financial or non-financial interests to disclose.

Data availability and materials

Not applicable.

References

1. Al-Jabri, K. S., Al-Saidy, A. H., and Taha, R. (2011). “Effect of copper slag as a fine aggregate on the properties of cement mortars and concrete.” *Construction and Building Materials*, 25(2), 933–938.
2. Al-Jabri, K. S., Hisada, M., Al-Oraimi, S. K., and Al-Saidy, A. H. (2009). “Copper slag as sand replacement for high performance concrete.” *Cement and Concrete Composites*, Elsevier, 31(7), 483–488.
3. American Society of Testing and Materials. (2014). “ASTM C136/C136M - 19: Standard Test Method for Sieve Analysis of Fine and Coarse Aggregates.” *Annual Book of ASTM Standards*.
4. Andrew, R. M. (2017). “Global CO₂ emissions from cement production.” *Earth System Science Data Discussions*, 1–52.
5. Ariffin, M. A. M., Bhutta, M. A. R., Hussin, M. W., Mohd Tahir, M., and Aziah, N. (2013). “Sulfuric acid resistance of blended ash geopolymer concrete.” *Construction and Building Materials*.
6. ASTM C1202. (2012). “Standard Test Method for Electrical Indication of Concrete’s Ability to Resist Chloride Ion Penetration.” *American Society for Testing and Materials.*, (C).
7. ASTM C143/C143M. (2015). “Standard Test Method for Slump of Hydraulic-Cement Concrete.” *Astm C143*, (1).
8. ASTM C1585-13. (2013). “Standard Test Method for Measurement of Rate of Absorption of Water by Hydraulic Cement Concretes.” *ASTM International*.
9. ASTM C642-13. (2013). “Standard test method for density, absorption, and voids in hardened concrete, ASTM International.” *ASTM International*.
10. ASTM International. (2020). “Standard Test Method for Compressive Strength of Cylindrical Concrete Specimens 1.” *ASTM*.
11. Behera, M., Minocha, A. K., and Bhattacharyya, S. K. (2019). “Flow behavior, microstructure, strength and shrinkage properties of self-compacting concrete incorporating recycled fine aggregate.” *Construction and Building Materials*, Elsevier Ltd, 228, 116819.
12. “Benefits of Statistical Modeling – Test Science.” (2015). <https://testscience.org/analyze-test-data/inferential/benefits-of-statistical-modeling/> (Apr. 4, 2021).

13. Dhirendra Singhal, P., and Garg, A. (2017). “Behaviour of Fly Ash based Geopolymer Concrete in Fresh State.” *Indian Journal of Science and Technology*.
14. “Effect of Water Cement Ratio on Strength of Concrete – we civil engineers.” (2017). <https://wecivilengineers.wordpress.com/2017/10/06/water-cement-ratio/> (Feb. 27, 2021).
15. Gagg, C. R. (2014). “Cement and concrete as an engineering material: An historic appraisal and case study analysis.” *Engineering Failure Analysis*.
16. Gardiner, A., and MacDonald, K. (2013). “Aggregate Moisture in Concrete| Concrete Construction Magazine.” <https://www.concreteconstruction.net/business/producers/aggregate-moisture-in-concrete_o> (Nov. 14, 2021).
17. Gorai, B., Jana, R. K., and Premchand. (2003). “Characteristics and utilisation of copper slag - A review.” *Resources, Conservation and Recycling*, Elsevier, 39(4), 299–313.
18. Gupta, N., and Siddique, R. (2020a). “Durability characteristics of self-compacting concrete made with copper slag.” *Construction and Building Materials*, Elsevier Ltd, 247, 118580.
19. Gupta, N., and Siddique, R. (2020b). “Durability characteristics of self-compacting concrete made with copper slag.” *Construction and Building Materials*, Elsevier Ltd, 247.
20. Guru Jawahar, J., Sashidhar, C., Ramana Reddy, I. V., and Annie Peter, J. (2013). “Micro and macrolevel properties of fly ash blended self compacting concrete.” *Materials and Design*, Elsevier, 46, 696–705.
21. Hanio Merinkline, H., Manjula Devi, S., and Christy, F. (2013). *Fresh And Hardened Properties Of Fly Ash Based Geopolymer Concrete With Copper Slag*. *International Journal of Engineering Research & Technology*, IJERT-International Journal of Engineering Research & Technology.
22. Imtiaz, L., Kashif, S., Rehman, U., Memon, S. A., Khan, M. K., and Javed, M. F. (2020). “A Review of Recent Developments and Advances in Eco-Friendly Geopolymer Concrete.”
23. IS:3812, and BIS 3812. (2013). “Specification for Pulverized fuel ash, Part-1: For Use as Pozzolana in Cement, Cement Mortar and Concrete.” *Bureau of Indian Standards, New Delhi, India*.
24. IS 383. (2016). “Coarse and fine aggregate for concrete - Specification.” *Bureau of Indian Satandards*.
25. Jindal, B. B., Jangra, P., and Garg, A. (2020). “Effects of ultra fine slag as mineral admixture on the compressive strength, water absorption and permeability of rice husk ash based geopolymer concrete.” *Materials Today: Proceedings*.
26. Jindal, B. B., Jindal, B. B., Singhal, D., Sharma, S. K., and Parveen. (2017). “Suitability of Ambient-Cured Alccofine added Low-Calcium Fly Ash-based Geopolymer Concrete.” *Indian Journal of Science and Technology*.
27. Khan, K. A., Raut, A., Chandrudu, C. R., and Sashidhar, C. (2021). “Design and development of sustainable geopolymer using industrial copper byproduct.” *Journal of Cleaner Production*, Elsevier, 278, 123565.
28. Kumar Tiwary, A., and Bhatia, S. (2021). “A study incorporating the influence of copper slag and fly ash substitutions in concrete.” *Materials Today: Proceedings*, Elsevier.

29. Mahendran, K., and Arunachelam, N. (2016). “Performance of Fly Ash and Copper Slag based Geopolymer Concrete.” *Indian Journal of Science and Technology*, Indian Society for Education and Environment, 9(2).
30. Mathew, N. S., and Usha, S. (2016). *Effects of Copper Slag as Partial Replacement for Fine Aggregate in Geopolymer Concrete*. *IOSR Journal of Mechanical and Civil Engineering*.
31. Mavroulidou, M. (2017a). “Mechanical Properties and Durability of Concrete with Water Cooled Copper Slag Aggregate.” *Waste and Biomass Valorization*, Springer Netherlands, 8(5), 1841–1854.
32. Mavroulidou, M. (2017b). “Mechanical Properties and Durability of Concrete with Water Cooled Copper Slag Aggregate.” *Waste and Biomass Valorization*, Springer Netherlands, 8(5), 1841–1854.
33. Mayhoub, O. A., Nasr, E. S. A. R., Ali, Y. A., and Kohail, M. (2021). “The influence of ingredients on the properties of reactive powder concrete: A review.” *Ain Shams Engineering Journal*, Elsevier, 12(1), 145–158.
34. Meyer, C. (2004). “Concrete Materials and Sustainable Development in the USA.” *Engineering International*, 203–207.
35. Mosaberpanah, M. A., and Eren, O. (2017). “Effect of quartz powder, quartz sand and water curing regimes on mechanical properties of UHPC using response surface modelling.” *Advances in Concrete Construction*, Techno Press, 5(5), 481–492.
36. Ng, H. T., Heah, C. Y., and Liew, Y. M. (2018). “The effect of various molarities of NaOH solution on fly ash geopolymer paste.” 2045, 20098.
37. Parveen, and Singhal, D. (2017). “Development of mix design method for geopolymer concrete.” *Advances in Concrete Construction*.
38. Parveen, Singhal, D., and Jindal, B. B. (2017). “Experimental study on geopolymer concrete prepared using high-silica RHA incorporating alccofine.” *Advances in Concrete Construction*, 5(4).
39. Parveen, Singhal, D., Junaid, M. T., Jindal, B. B., and Mehta, A. (2018a). “Mechanical and microstructural properties of fly ash based geopolymer concrete incorporating alccofine at ambient curing.” *Construction and Building Materials*, 180.
40. Parveen, Singhal, D., Junaid, M. T., Jindal, B. B., and Mehta, A. (2018b). “Mechanical and microstructural properties of fly ash based geopolymer concrete incorporating alccofine at ambient curing.” *Construction and Building Materials*.
41. Prem, P. R., Verma, M., and Ambily, P. S. (2018). “Sustainable cleaner production of concrete with high volume copper slag.” *Journal of Cleaner Production*, Elsevier Ltd, 193, 43–58.
42. Rahmani, K., Shamsai, A., Saghafian, B., and Peroti, S. (2012). “Effect of Water and Cement Ratio on Compressive Strength and Abrasion of Microsilica Concrete.” *Middle-East Journal of Scientific Research*, 12(8), 1056–1061.
43. Rathanasalam, V., Perumalsami, J., and Jayakumar, K. (2020). “Characteristics of Blended Geopolymer Concrete Using Ultrafine Ground Granulated Blast Furnace Slag and Copper Slag.” *Annales de Chimie - Science des Matériaux*, International Information and Engineering Technology Association, 44(6), 433–439.

44. Rohith, R., Kumar, R. V., Nagajothi, S., and Elavenil, S. (2018). “Experimental Investigation of Geopolymer Concrete Using Metakaolin and Copper Slag.” 10(Special Issue 08-Special Issue), 612–615.
45. Saloni, Parveen, Pham, T. M., Lim, Y. Y., Pradhan, S. S., Jatin, and Kumar, J. (2021). “Performance of rice husk Ash-Based sustainable geopolymer concrete with Ultra-Fine slag and Corn cob ash.” *Construction and Building Materials*, Elsevier Ltd, 279, 122526.
46. Saloni, Singh, A., Sandhu, V., Jatin, and Parveen. (2020). “Effects of alccofine and curing conditions on properties of low calcium fly ash-based geopolymer concrete.” *Materials Today: Proceedings*.
47. “Saturated-surface-dry - Wikipedia.” (2018). <https://en.wikipedia.org/wiki/Saturated-surface-dry> (Oct. 31, 2021).
48. Singh, A., and Mehta, S. (2020). “Partial Replacement of Fine Aggregate With Copper Slag And Marble Dust Powder In Geo-Polymer Concrete: A Review.” *International Research Journal of Engineering and Technology*.
49. SivaranjaniS, and Sridhar M. (2019). *Strength and Durability Study of Geopolymer Concrete With 100% Replacement of Sand Using Copper Slag*.
50. *Specification and Guidelines for Self-Compacting Concrete*. (2002). .
51. Sreenivasulu, C., Guru Jawahar, J., and Sashidhar, C. (2020). “Effect of Copper Slag on Micro, Macro, and Flexural Characteristics of Geopolymer Concrete.” *Journal of Materials in Civil Engineering*.
52. Teo, D., Lee, C., and Lee, T. S. (2016). “The effect of aggregate condition during mixing on the mechanical properties of oil palm shell (OPS) concrete.” *MATEC Web of Conferences*.
53. *The European Guidelines for Self-Compacting Concrete Specification, Production and Use “The European Guidelines for Self Compacting Concrete.”* (2005). .
54. Un, C. H. (2017). *Creep Behaviour of Geopolymer Concrete*.
55. Xie, J., and Kayali, O. (2016). “Effect of superplasticiser on workability enhancement of Class F and Class C fly ash-based geopolymers.” *Construction and Building Materials*, Elsevier Ltd, 122, 36–42.
56. Xu, A., and Shayan, A. (2016). “Effect of activator and water to binder ratios on setting and strength of geopolymer concrete.”
57. Yakshareddy, B., Guru Jawahar, J., Sreenivasulu, C., and Sashidhar, C. (2018). *Preliminary Study on Geopolymer Concrete using Copper Slag and Vermiculite*. *International Journal of Research and Scientific Innovation (IJRSI) |*.

Figures

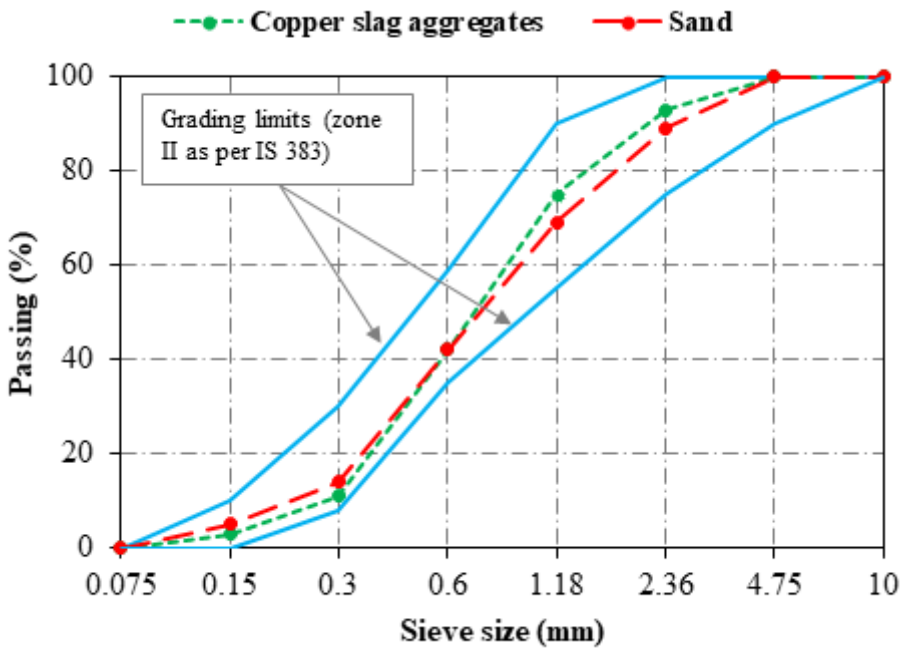

Figure 1

Particle size distribution curve for aggregates

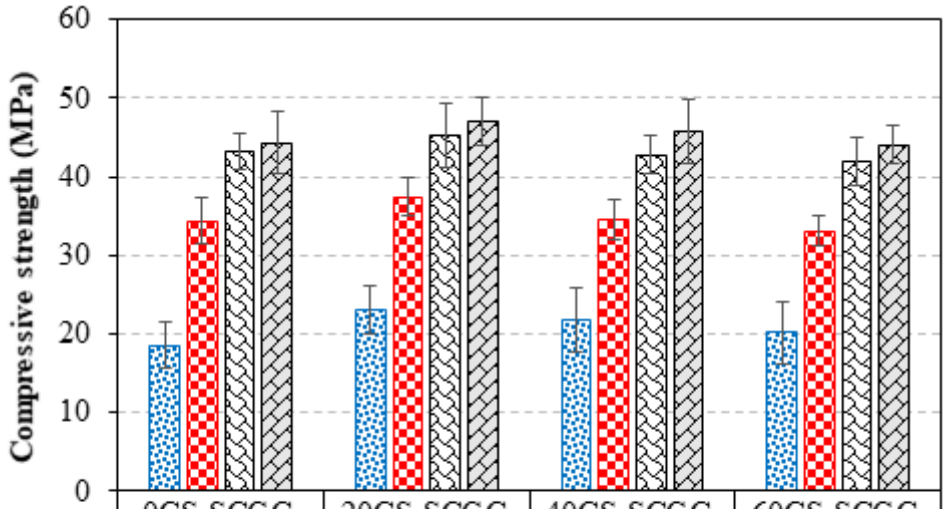

	0CS-SCGC	20CS-SCGC	40CS-SCGC	60CS-SCGC
7 days	18.56	23.12	21.75	20.19
28 days	34.38	37.42	34.58	33.10
90 days	43.18	45.22	42.76	41.96
365 days	44.27	47.03	45.73	44.06

Figure 2

Compressive strength of various SCGC mixes.

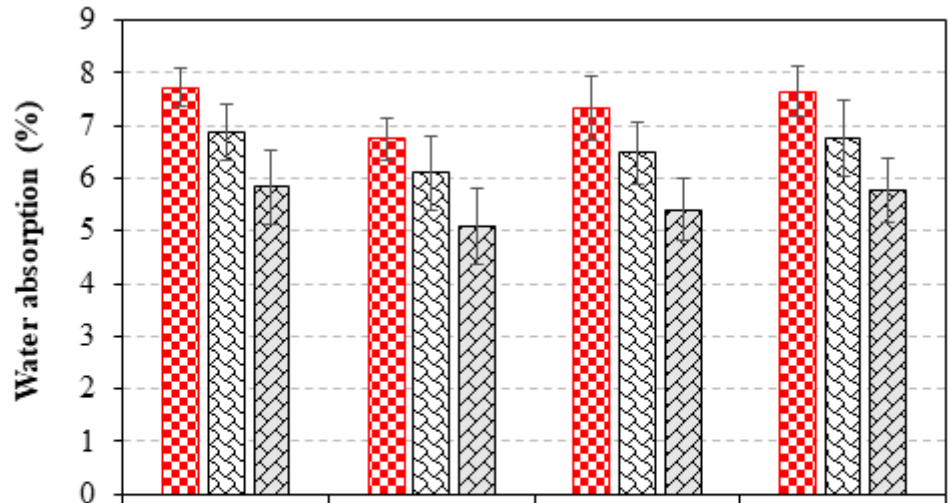

	0CS-SCGC	20CS-SCGC	40CS-SCGC	60CS-SCGC
28 days	7.71	6.74	7.33	7.64
90 days	6.86	6.10	6.48	6.77
365 days	5.83	5.08	5.40	5.76

Figure 3

Water absorption of SCGC mixes.

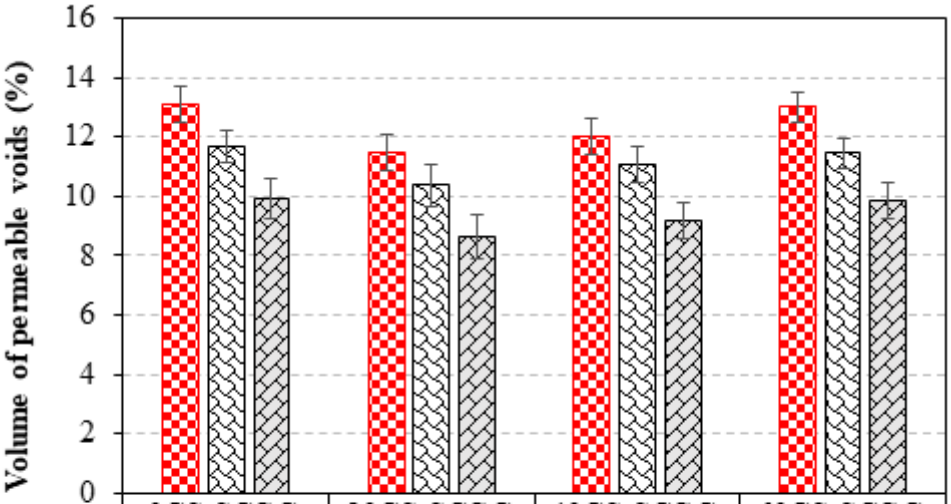

	0CS-SCGC	20CS-SCGC	40CS-SCGC	60CS-SCGC
28 days	13.11	11.46	12.01	12.99
90 days	11.66	10.37	11.05	11.45
365 days	9.91	8.64	9.18	9.85

Figure 4

Volume of permeable voids of SCGC mixes.

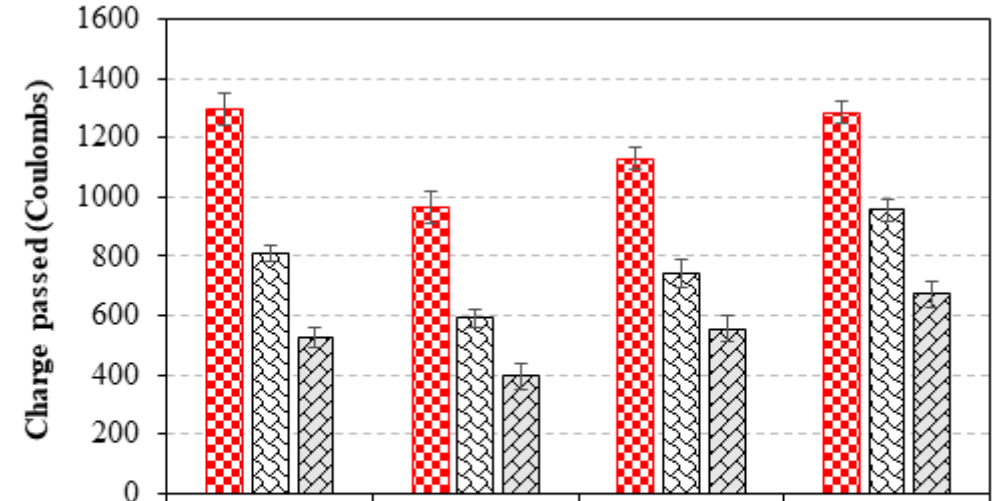

	0CS-SCGC	20CS-SCGC	40CS-SCGC	60CS-SCGC
28 days	1293	963	1130	1284
90 days	811	590	742	955
365 days	526	394	554	672

Figure 5

RCPT results of SCGC mixes.

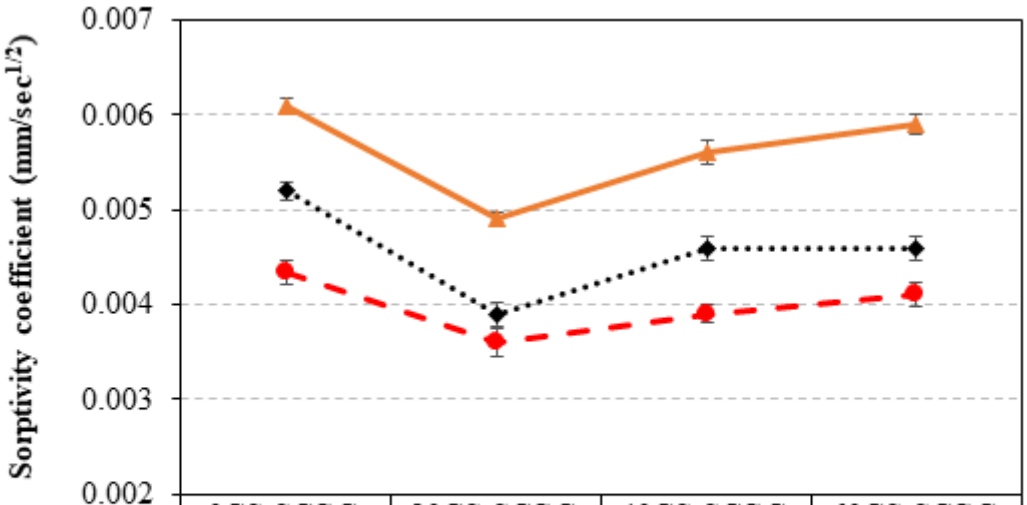

	0CS-SCGC	20CS-SCGC	40CS-SCGC	60CS-SCGC
28 days	0.0061	0.0049	0.0056	0.0059
90 days	0.0052	0.0039	0.0046	0.0046
365 days	0.0043	0.0036	0.0039	0.0041

Figure 6

Sorptivity coefficients of SCGC mixes.

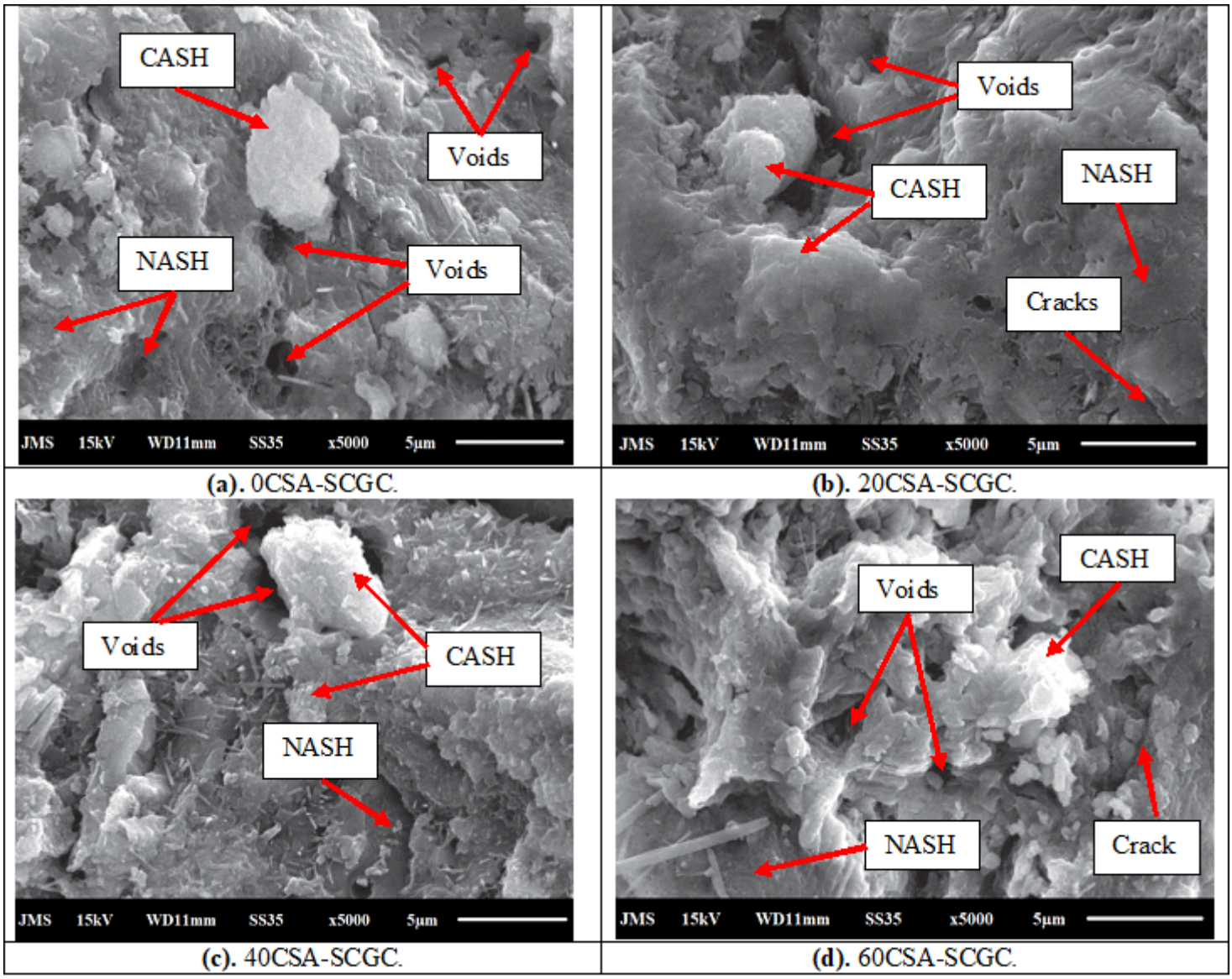

Figure 7

Microstructure of various SCGC mixes at the age of 90 days.

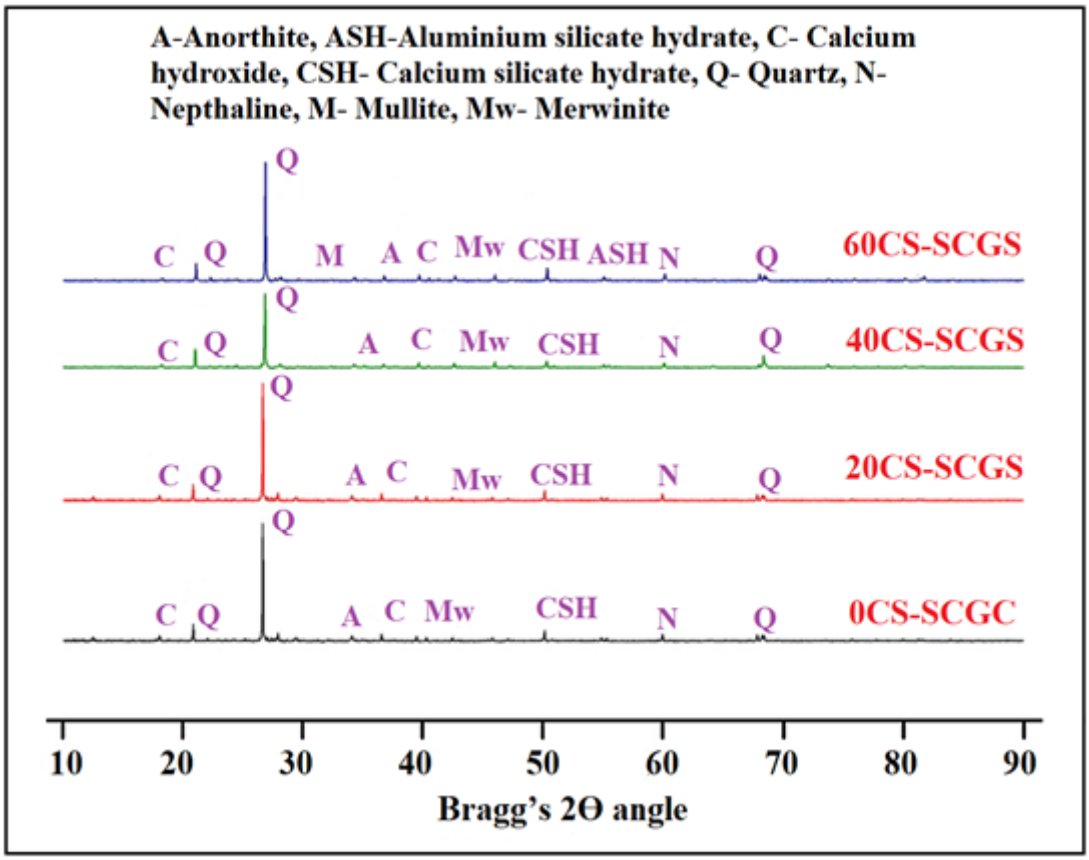

Figure 8

XRD analysis of SCGC mixes at the age of 90 days.

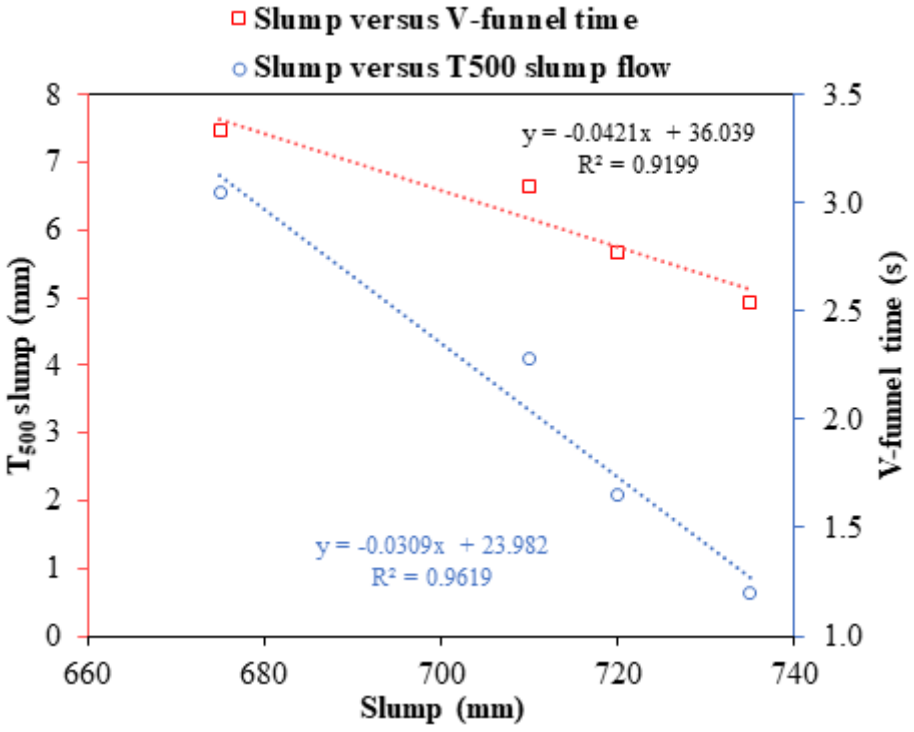

Figure 9

Relationship of slump with T_{500} slump flow and V-funnel time of SCGC mixes.

Note: The equations obtained are valid for the below mentioned range of the parameters:

Slump (mm): 675 – 735

T500 slump flow (s): 1.20 – 3.05

V-funnel time (s): 4.92 – 7.48

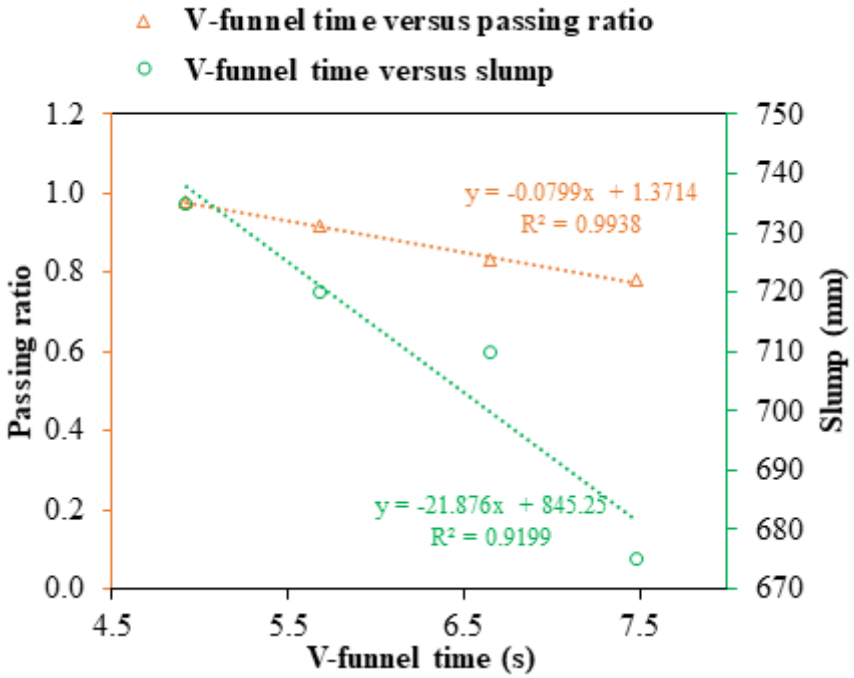

Figure 10

Relationship of V-funnel time with passing ratio and slump of SCGC mixes.

Note: The equations obtained are valid for the below mentioned range of the parameters:

V-funnel time (s): 4.92 – 7.48

Passing ratio: 0.78 – 0.98

Slump (mm): 675 – 735

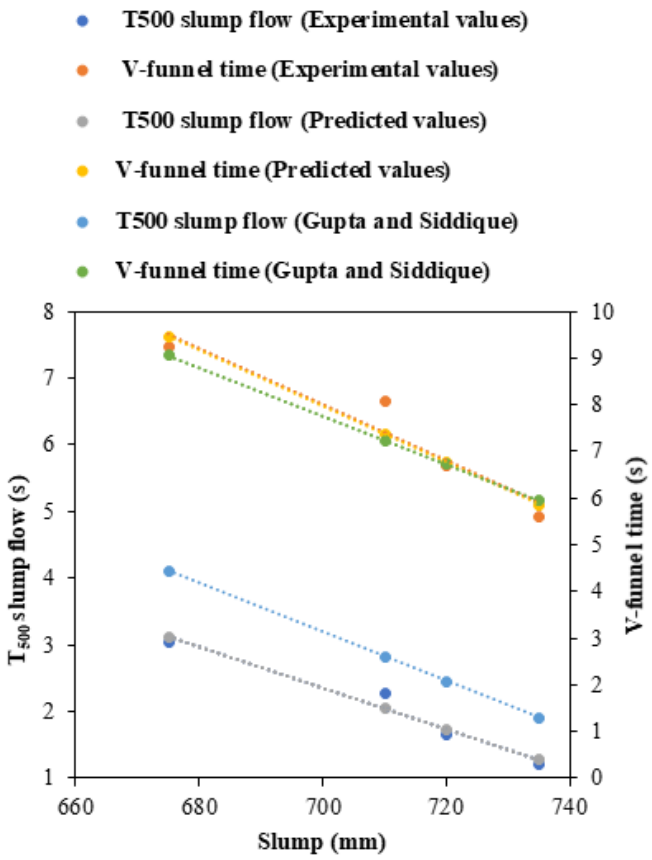

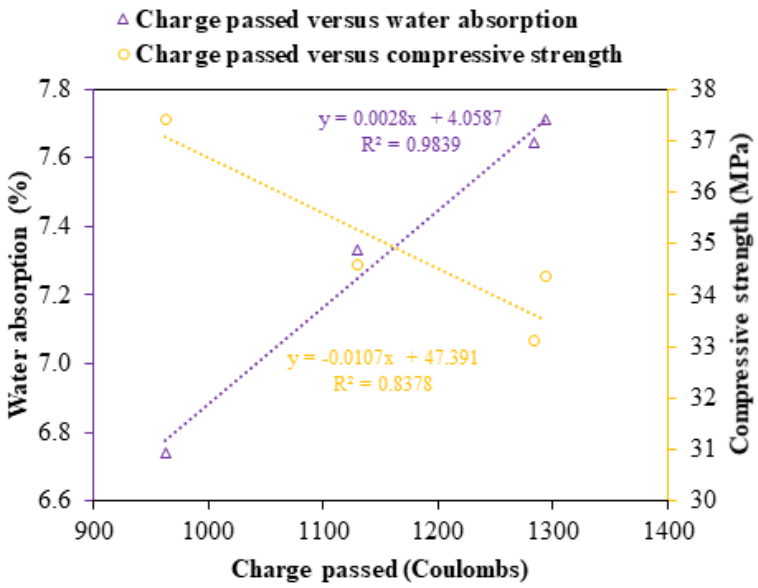

Figure 11

Relationship of compressive strength with charge passed and water absorption

of SCGC mixes.

Note: The equations obtained are valid for the below mentioned range of the parameters:

Charge passed (Coulombs): 963 – 1293

Water absorption (%): 6.74 – 7.71

Compressive strength (MPa): 33.10 – 34.38